

SCALING CRITERIA FOR THE DEVELOPMENT OF AN ACOUSTICALLY STABILIZED DUMP COMBUSTOR

JERALD A. COLE,¹ TIMOTHY P. PARR,² NEIL C. WIDMER,¹ KENNETH J. WILSON,²
KLAUS C. SCHADOW² AND WM. RANDALL SEEKER²

¹*GE Energy and Environmental Research Corporation
Irvine, California, USA*

²*Naval Air Warfare Center, Weapons Division
China Lake, California, USA*

Acoustic stabilization of combustion in a dump configuration results in completion of combustion in a relatively short residence time with simultaneously low emissions of oxides of nitrogen, carbon monoxide, and hydrocarbons. Acoustically stabilized combustion is also a potential means for achieving closed-loop active control of combustion. Therefore, a promising burner configuration identified through laboratory bench-top experiments was developed and scaled up for application as an afterburner for a starved-air incinerator with the objective of providing a compact device capable of achieving pollutant emissions performance better than required by current International Maritime Organization regulations. In the absence of established scaling criteria, factors governing vortex generation and jet mixing theory were examined. These provided useful guidelines for burner design as the dump combustor was successively scaled up from a 4.75 kW laboratory experiment to a nominal 700 kW unit tested on a starved-air incinerator. Key parameters considered were the central air jet velocity, jet diameter (and area) acoustic driving frequency, and characteristic jet mixing time. Burner performance was maintained or improved as both jet velocity and jet area were increased approximately as the square root of burner scale. This resulted in increases in the acoustic driving frequency and burner pressure drop with scale, which have implications for development of even larger burners using this technology.

Initial development was conducted using simulated low-Btu gas mixtures at ambient temperature. Application as an afterburner required hardware modifications to accommodate higher gas volumes at higher temperatures. Despite significant changes in burner geometry, coherent vortex generation was established by acoustic excitation and continued to effect reductions in NO_x and CO emissions. The higher combustion temperatures encountered with hot simulated and real pyrolysis products led to higher CO and NO_x emissions, but emission performance continued to exceed applicable regulatory guidelines by a substantial margin.

Introduction

An acoustically stabilized vortex burner was developed as part of a program focusing on high firing density, wide flammability limits, and stable combustion [1]. An acoustic signal was used to force a central combustion air jet entering a dump combustor in order to trip the periodic formation of coherent annular vortices and enhance the jet mixing rate [2,3]. A fuel stream was introduced annularly around the central air jet. Burner performance was studied using visualization, gas sampling, and pneumoacoustic measurements [4]. Laboratory tests were conducted with 4.75 and 47 kW burners. The burner was then successively scaled up to a nominal 700 kW and tested as an afterburner for a starved-air primary waste incinerator.

Background

In the classic dump combustor, flame stability is achieved through backmixing of hot combustion

products into the shear layer of the jet. Mixing with the entrained products is enhanced by the formation of annular vortices surrounding the central jet at the dump plane. These vortices are produced at an average rate described by the expression

$$f = St \times \frac{U_e}{d_j} \quad (1)$$

where f is the preferred frequency of the jet; St is the preferred Strouhal number, with a typical range of 0.25 to 0.5 [5]; U_e is the jet exit velocity; and d_j is the jet diameter.

The significance of equation 1 is illustrated by Fig. 1 where the unforced curve shows the power spectrum of the central air jet velocity in a 47 kW acoustic burner measured by hot wire anemometry. The maximum of this curve corresponds to the preferred frequency of vortex formation. Acoustic excitation of the jet at this frequency produced the forced curve

Report Documentation Page

Form Approved
OMB No. 0704-0188

Public reporting burden for the collection of information is estimated to average 1 hour per response, including the time for reviewing instructions, searching existing data sources, gathering and maintaining the data needed, and completing and reviewing the collection of information. Send comments regarding this burden estimate or any other aspect of this collection of information, including suggestions for reducing this burden, to Washington Headquarters Services, Directorate for Information Operations and Reports, 1215 Jefferson Davis Highway, Suite 1204, Arlington VA 22202-4302. Respondents should be aware that notwithstanding any other provision of law, no person shall be subject to a penalty for failing to comply with a collection of information if it does not display a currently valid OMB control number.

1. REPORT DATE 04 AUG 2000	2. REPORT TYPE N/A	3. DATES COVERED -	
4. TITLE AND SUBTITLE Scaling Criteria for the Development of an Acoustically Stabilized Dump Combustor		5a. CONTRACT NUMBER	
		5b. GRANT NUMBER	
		5c. PROGRAM ELEMENT NUMBER	
6. AUTHOR(S)		5d. PROJECT NUMBER	
		5e. TASK NUMBER	
		5f. WORK UNIT NUMBER	
7. PERFORMING ORGANIZATION NAME(S) AND ADDRESS(ES) GE Energy and Environmental Research Corporation Irvine, California, USA		8. PERFORMING ORGANIZATION REPORT NUMBER	
9. SPONSORING/MONITORING AGENCY NAME(S) AND ADDRESS(ES)		10. SPONSOR/MONITOR'S ACRONYM(S)	
		11. SPONSOR/MONITOR'S REPORT NUMBER(S)	
12. DISTRIBUTION/AVAILABILITY STATEMENT Approved for public release, distribution unlimited			
13. SUPPLEMENTARY NOTES See also ADM001790, Proceedings of the Combustion Institute, Volume 28. Held in Edinburgh, Scotland on 30 July-4 August 2000.			
14. ABSTRACT			
15. SUBJECT TERMS			
16. SECURITY CLASSIFICATION OF:			17. LIMITATION OF ABSTRACT
a. REPORT unclassified	b. ABSTRACT unclassified	c. THIS PAGE unclassified	UU
			18. NUMBER OF PAGES 8
			19a. NAME OF RESPONSIBLE PERSON

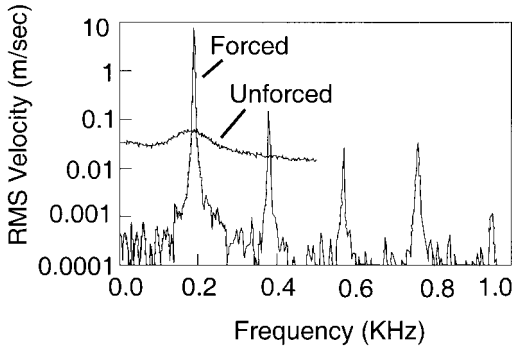


FIG. 1. Measurements of the power spectrum of the central air jet's root mean square velocity in a 47 kW dump combustor under forced and unforced operation.

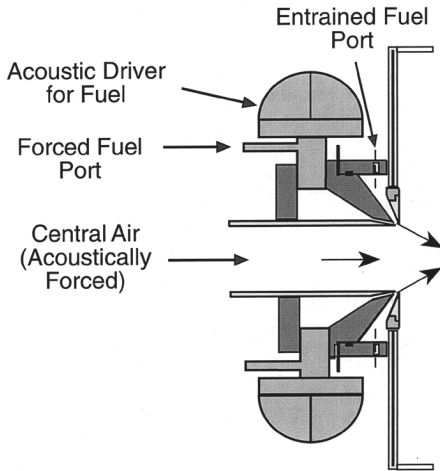


FIG. 2. Illustration of the 4.75 kW acoustic burner firing into a dump combustor. The burner is equipped with an acoustically forced central air jet and both forced and entrained fuel injection annuli. Essentially equivalent designs were used for the 47 kW and 330 kW burner.

in which the majority of the energy at non-preferred frequencies has vanished. Under these conditions, mixing of the jet with the surroundings is caused not by momentum effects (Reynolds number), but rather by shear in the acoustically induced coherent vortex. A compact high-firing-density combustor was developed around the enhanced mixing of these large-scale vortical structures [6-8], which enable the external mixing of fuel and air while producing a flame with visual and pollutant emissions characteristics similar to premixed flames.

Laboratory-Scale Development

Features of the 4.75 kW acoustically stabilized vortex burner are illustrated in Fig. 2. Details are

discussed later. Composite planar laser-induced fluorescence in-flame mapping of the near-field (50 mm) mixing between the central air jet and fuel [9] showed that fuel rolls up into the vortex between the air and the entrained hot combustion products. Ignition of the combustible mixture is delayed due to high local strain rate [10,11] until substantial mixing of the three gases has occurred, leaving a lifted flame with no evidence of diffusion flame character. Combustion was essentially complete within 400 ms.

The scale-up of this burner required the development of scaling criteria. To begin this development, a scale factor *S* was defined as

$$S = \frac{Q'}{Q} \tag{2}$$

where *Q* is the central air jet volumetric flow rate at 4.75 kW, and the prime indicates properties at a given scale.

Jet velocity *U_e* and jet area *A_j* are related to *Q* by *Q* = *U_e* × *A_j* where

$$A_j = \frac{\pi}{4} d_j^2$$

From this, the following relationships are derived:

$$Q = U_e \frac{\pi}{4} d_j^2, S = \frac{U'_e d'_j{}^2}{U_e d_j^2}$$

and

$$\frac{f'}{f} = \frac{St' U'_e d_j}{St U_e d'_j}$$

but

$$\frac{St'}{St} \sim 1$$

therefore

$$\frac{f'}{f} = S \frac{d_j^3}{d'_j{}^3}$$

In traditional burner scaling, a constant jet velocity is often maintained. Classical jet theory, however, suggests that increased jet velocity is needed to maintain the mixing rate. The mixing rate can be expressed in terms of the jet's well-mixed ratio *Wm* and the Ricou-Spalding entrainment equation as follows [12]:

$$Wm = c \times \left(\frac{\rho_p}{\rho_j}\right)^{1/2} \times \frac{S_x}{d_j} \tag{3}$$

where *c* is a measured constant, *S_x* is the characteristic well-mixed jet length, *ρ_j* is the density of the jet fluid, and *ρ_p* is the density of the entrained fluid.

Defining a characteristic jet mixing time as

$$\tau = \frac{S_x}{U_e} \quad (4)$$

then, from equations 3 and 4,

$$\tau = \frac{1}{c} \times Wm \times \left(\frac{\rho_i}{\rho_p}\right)^{1/2} \times \frac{d_i}{U_e} \quad (5)$$

Assuming the Wm , ρ_p , and ρ_i are constant, τ becomes a function of d_i/U_e .

For a constant mixing time

$$\frac{\tau'}{\tau} = 1 = \left(\frac{d_i'}{d_i}\right)^3 \times \frac{Q}{Q'}$$

so

$$\left(\frac{d_i'}{d_i}\right)^3 = \frac{Q'}{Q} = S$$

and

$$\frac{d_i'}{d_j} = S^{1/3} \quad (6)$$

Equation 6 is the jet diameter scaling criterion for a constant jet-mixing rate and for constant jet natural frequency. Jet velocity also scales by $S^{1/3}$ since

$$\frac{Q'}{Q} = \frac{U_e'}{U_e} \times \left(\frac{d_i'}{d_i}\right)^2$$

and

$$\begin{aligned} \frac{U_e'}{U_e} &= \frac{Q'}{Q} \times \left(\frac{d_i}{d_i'}\right)^2 = S \times S^{-2/3} \\ \frac{U_e'}{U_e} &= S^{1/3} \end{aligned} \quad (7)$$

In summary, scaling velocity by an exponential factor below 1/3 results in slower jet mixing and above 1/3 results in faster jet mixing.

While this development explains possible consequences of any particular scaling criteria, no basis is established for the selection of scaling criteria. However, there exist practical issues that impact the choice of scaling criteria.

Inlet Air Velocity

Constant velocity scaling criterion will, according to the Ricou–Spaulding analysis, lead to a reduced rate of jet mixing in the absence of acoustics. If constant jet mixing time is to be maintained, velocity must increase with at least the 1/3 power of scale. However, at some point, increased velocity will impose an unacceptable level of pressure drop on the system.

Jet Mixing Time

Hypotheses proposed to explain operation of the burner suggest that enhanced mixing is key to emissions performance at the 4.75 kW scale. At a minimum, therefore, it is preferred that the characteristic

mixing time not increase greatly and, if possible, stay at least constant.

Frequency

While acoustics are known to play a key role in performance, the role of frequency is not understood. In work conducted at the 4.75 kW scale, the frequency could be varied by a factor of two above and below the preferred mode before any degradation of performance was noted. However, others [13] have observed that acoustically induced improvements in combustion performance were reduced as frequencies increased toward 800 Hz, possibly as a result of a diminished pressure amplitude at higher resonant frequencies [14,15]. It is also a concern that at very low frequencies the slow vortex shedding rate could reduce strain rate during vortex rollup, leading to momentum-dominated mixing and premature ignition.

Addressing these concerns, scaling was conducted by increasing jet velocity and jet area approximately equally. Relating jet area and velocity to flow rate and substituting this into equation 2,

$$\frac{U_e'}{U_e} = S^{1/2} \quad (8)$$

$$\frac{A_j'}{A_j} = S^{1/2} \quad (9)$$

$$\frac{d_i'}{d_j} = S^{1/4} \quad (10)$$

This results in the jet velocity increasing at a greater rate than the jet diameter and drives changes in jet characteristics such as natural resonant frequency and Ricou–Spaulding mixing rate.

As scale increases, the jet Reynolds number increases as $S^{3/4}$ and natural frequency as $S^{1/4}$ while the characteristic jet mixing time decreases as $S^{-1/4}$.

Overview of Scaling Efforts

Four distinct burner sizes were tested at nominal scale factors of 1, 10, 100, and 150 using the 4.75 kW burner as the reference scale. Table 1 provides details of the different burners tested. Table 1 also shows how the actual combustor size and gas residence time changed with scale. The 4.75, 47, and 330 kW burners were essentially identical, having the features illustrated in Fig. 2. The size of the annular fuel injection nozzle was chosen so that the axial component of the fuel velocity roughly matched that of the central air jet.

The 47 kW burner had a central air jet velocity of 10.3 m/s issuing from a 38.4 mm diameter nozzle. The natural jet frequency, corresponding to a Strouhal number of 0.41, is 120 Hz. The burner fired into

TABLE 1
Summary of burner scales and scaling parameters for the acoustic burner development program

	Scale Factor ^a				
	1	10	82	96	147
Total heat input (kW)	4.75	47	330	510	700
Fuel heat input ^b (kW)	4.75	47	330	315	450
Jet air flow (m ³ /h)	4.52	42.9	369	432	663
Jet diameter (mm)	22	38.4	66.0	71.4	81.8
Jet velocity (m/s)	3.3	10.3	30.0	30.0	35.0
Design jet velocity (m/s)	3.3	10.2	30.2	32.7	40.5
Actual exponential scaling factors:					
for diameter ^c	—	0.247	0.249	0.258	0.263
for velocity ^d	—	0.505	0.501	0.484	0.474
Combustor characteristics:					
Diameter (mm)	120	178	584	356	345
Length (mm)	420	534	1000	1067	1370
Residence time (ms)	~500	~150	~300	86	68

Note: The actual exponential scaling factors for jet diameter and velocity closely match the design scaling criteria where jet area and velocity are scaled proportionally by the exponential factor of 0.5.

^aScaling factor based on jet airflow.

^bExcludes sensible heat for hot pyrolyzed gases.

^cThe selected scaling criteria exponential factor is 0.25.

^dThe selected scaling criteria exponential factor is 0.50.

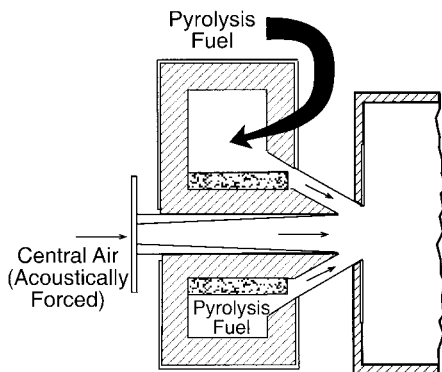


FIG. 3. Illustration of the 510 kW burner designed for afterburner operation.

a sudden expansion chamber of 178 mm diameter and 550 mm length.

Nominal 330 kW System

Cold fuel tests were conducted on a nearly full-scale afterburner that operated nominally at 330 kW. These tests were conducted with a fuel comprised of ethylene and nitrogen and included direct fuel modulation. The design was a direct scale-up of the 47 kW unit and resulted in a 67 mm jet diameter

with the jet issuing at 30 m/s into a 584 mm combustor diameter of 1000 mm length.

510 kW System

At the 510 kW scale, the introduction of hot pyrolysis gases as fuel required a significant increase in the dimensions of the plenae and channels used to convey the fuel in order to avoid excessive pressure drop and to maintain velocity matching between the fuel and air [16]. Details of this new geometry are illustrated in Fig. 3. The combustion chamber was 356 mm diameter and 1067 mm long, with a gas residence time of 86 ms.

Nominal 700 kW System

Tests at the 510 kW scale showed excessive pressure drop through the fuel plenae. As a result, the 700 kW burner (Fig. 4) was equipped with ejectors using tapered elliptic nozzles [17] to entrain pyrolysis products into the combustion zone. The burner air jet velocity was 35 m/s with an 81.8 mm diameter nozzle. The combustion chamber was 345 mm diameter and 1370 mm length, with an average residence time of 68 ms at the gas sampling location.

Results

The 4.75 kW burner was initially tested using ethylene fuel with benzene added at 7 vol % to act as

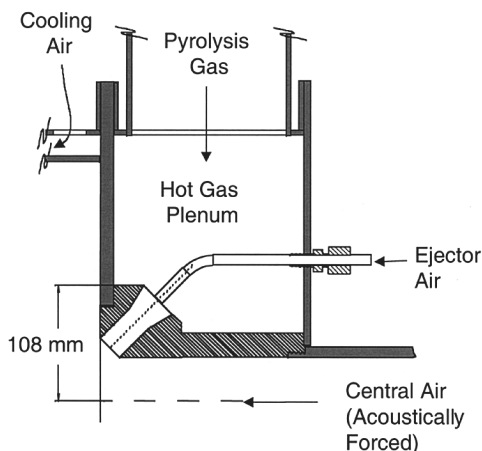


FIG. 4. Illustration of the 700 kW burner designed for afterburner operation. The burner employs entrained fuel injection through 12 mm diameter fuel injector jets that are located around the forced central air jet. The fuel inlets are equipped with ejector air to aid pumping of fuel to reduce pressure drop.

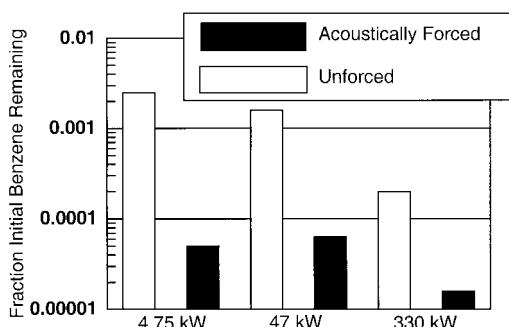


FIG. 5. Destruction efficiency of spiked benzene in cold fuel tests on the 4.75, 47, and 330 kW burners. Actual firing rates during these tests were 4.75, 35, and 280 kW.

an indicator of combustion efficiency. The 47 and 330 kW burners were tested using a simulated medium-Btu gas consisting of nitrogen blended with ethylene and benzene. Fig. 5 shows how benzene destruction and removal efficiency (DRE) varied with burner scale and with and without acoustic forcing. At the 4.75 kW scale, DRE improved from 99.75% to 99.995% due to acoustic forcing. This laboratory burner was fired into a relatively large chamber providing 0.5 s of gas residence time.

The 47 kW burner fired into a chamber that provided only around 150 ms of gas residence time. Despite the reduced residence time, the benzene DRE reached 99.994% with acoustic forcing compared to only 99% without. Measurements also showed that carbon monoxide emission dropped from 800 ppm

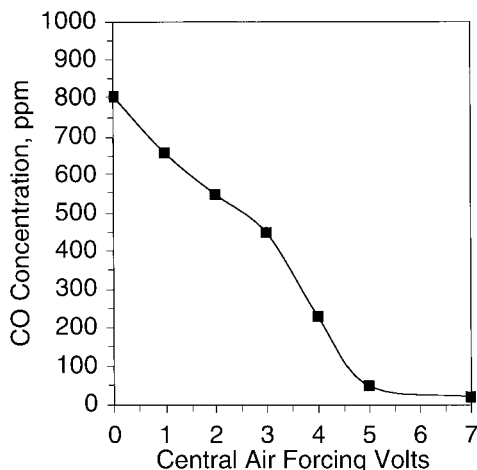


FIG. 6. CO concentrations for the 47 kW burner at varying central air forcing power levels. A voltage level of 7 V corresponds to a forcing power of only 5 W.

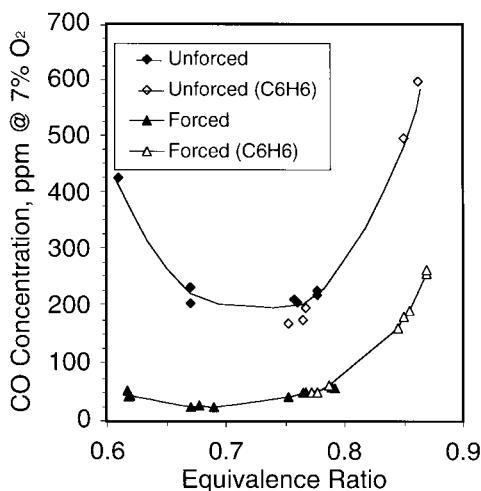


FIG. 7. In-chamber CO levels at varying equivalence ratio for forced and unforced operation of the 330 kW burner. The fuel consisted of 34% ethylene and 66% nitrogen mixture, and in noted cases (C₆H₆) benzene was spiked at 7% by weight.

to below 20 ppm as forcing power was increased from 0 to 7 V (Fig. 6).

The 330 kW burner design resembled the smaller burners in every aspect from knife-edged injector slots to an acoustically forced fuel stream. The performance of the 330 kW burner was similarly impressive. CO emissions were optimized below 20 ppm and benzene destruction of 99.998% was achieved with acoustic forcing. At an equivalence ratio of 0.67, acoustic forcing (Fig. 7) reduced CO emissions from over 200 ppm to below 20 ppm.

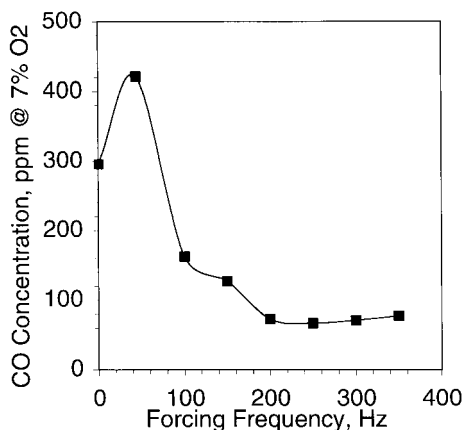


FIG. 8. The 510 kW burner in-chamber CO levels at varying acoustic forcing frequencies.

TABLE 2
Operational parameters for the 700 kW burner firing on hot simulated pyrolysis gas

	Turndown (%)		
	66	100	133
Jet air flow (m ³ /h)	333	500	666
Jet diameter (mm)	81.8	81.8	81.8
Jet velocity (m/s)	30	45	60
Frequency (Hz)	240	240	240
Strouhal no.	0.66	0.44	0.033
Actual exponential scaling factors:			
for diameter ^a	0.272	0.251	0.238
for velocity ^b	0.456	0.498	0.525

Note: A factor of two overall turndown did not affect combustion stability. This is partially explained by the scaling factor for jet diameter and velocity, which change relatively little over the entire turndown range.

^aThe selected scaling criteria exponential factor is 0.25.

^bThe selected scaling criteria exponential factor is 0.50.

The natural destruction of benzene is seen to increase in these tests. This results from thermal feedback from the surroundings and increasing optical density of the reacting gas mixture. The effects of acoustics, while still significant at larger scales, appear to be diminished because of natural turbulence-driven mixing, which resists the effects of the acoustics.

At the 510 kW scale, it was not possible to acoustically force the hot pyrolysis gas fuel stream due to temperature limitations on the acoustic drivers. Nor could we spike the hot fuel stream with benzene. Indicators of performance then centered on CO

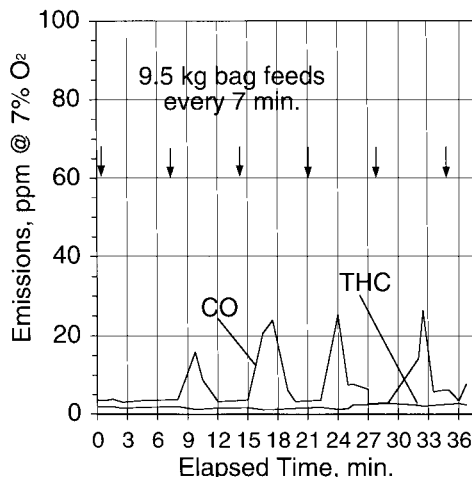


FIG. 9. Demonstrated emission performance of the 700 kW burner operating on pyrolyzed solid waste and auxiliary fuel from a commercial marine incinerator.

emissions. The hot pyrolysis gas produced by partial oxidation of ethylene in a precombustor was delivered to the burner at 375 °C. As a result, the combustion chamber was significantly hotter than in the smaller scale tests, leading to higher CO concentrations that did not fall below 60 ppm. The impact of forcing frequency and of forced and unforced operations is illustrated in Fig. 8. Under unforced operation ($f = 0$), the CO levels sampled 86 ms downstream of the burner were approximately 300 ppm. At the preferred mode frequency of 220 Hz CO levels were reduced to 70 ppm and unburned hydrocarbon concentrations were at the detection limit of 1 ppm.

The 700 kW burner was bench tested using simulated hot pyrolysis gas produced by burning ethylene under air-starved conditions. The burner operated with stable vortex combustion over varying central airflow rates corresponding to air jet velocities of 30, 45, and 60 m/s and scales of 125, 188, and 250 times the 4.75 kW burner. These operating conditions are presented in Table 2. The 700 kW burner would not operate without acoustic forcing of the central air jet.

The burner was fitted to the exhaust of a commercial waste incinerator to test its ability to operate under conditions of changing fuel flow rate and composition. The incinerator was fueled with a surrogate municipal solid waste consisting of plastic pellets and green waste. Emissions of CO and hydrocarbons during these tests are illustrated in Fig. 9. Arrows on the figure indicate when solid waste was fed to the incinerator. The burner equivalence ratio varied from 0.53 to 0.86, corresponding to variations in pyrolysis gas production. Despite these variations, average CO emissions were 8.5 ppm, unburned hydrocarbons were at the detection limit of 2 ppm, and

NO was below 100 ppm, all as measured 200 ms downstream of the burner. Also, while the waste pyrolysis gas contained a heavy soot loading, there were no visible soot emissions from the afterburner, and a filter in the gas sampling line showed no evidence of soot after 30 min of sample collection.

Discussion

An acoustically stabilized vortex burner was successfully scaled up from a 4.75 kW laboratory experiment to a 700 kW scale device used as an afterburner for a starved-air waste pyrolysis unit. Scaling was based on criteria described in equations 8, 9, and 10, in which central air jet velocity and jet area increase equally with burner scale factor S . At smaller scales where the burner concept was developed, exceptional emissions performance was obtained by acoustically forcing both the central combustion air jet and the fuel stream. At the larger 510 and 700 kW scales, use of hot pyrolysis gases as fuel precluded acoustically forcing the fuel stream. As a result, acoustic forcing did not provide the same improvements in performance seen at smaller scales. Nevertheless, the final full-scale burner design did operate stably during fluctuations in pyrolysis gas feed rate and composition with low emissions of CO, NO, and hydrocarbons.

Acknowledgments

Financial support for this work is provided by the Strategic Environmental Research and Development Program of the Joint Chiefs of Staff under contract N00014-96-C-0105. Dr. Klaus C. Schadow is the Project Technical Monitor.

REFERENCES

- Schadow, K. C., Hendricks, E. W., and Hansen, R. J., "Recent Progress in the Implementation of Active

Combustion Control," Eighteenth Congress of the International Council of the Aeronautical Sciences, Beijing, People's Republic of China, September 21–25, 1992.

- Oster, D., and Wygnanski, I. J., *J. Fluid Mech.* 123:91 (1982).
- Ho, C. M., and Haung, L. S., *J. Fluid Mech.* 119:443 (1982).
- Hanson, R. K., *Proc. Combust. Inst.* 21:1677–1691 (1986).
- Gutmark, E., and Ho, C. M., *Phys. Fluids* 26(10):2932 (1983).
- Crow, S. C., and Champagne, F. H., *J. Fluid Mech.* 48:545 (1971).
- Brown, G. L., and Roshko, A., *J. Fluid Mech.* 64:775 (1974).
- Ho, C. M., and Huerre, P., *Annu. Rev. Fluid Mech.* 16:365 (1984).
- Parr, T. P., Gutmark, E. J., Wilson, K. J., Hanson-Parr, D. M., Yu, K., Smith, R. A., and Schadow, K. C., *Proc. Combust. Inst.* 26:2471–2477 (1996).
- Keller, J. O., Barr, P. K., and Gemmen, R. S., *Combust. Flame* 99:29–42 (1994).
- Barr, P. K., and Keller, J. O., *Combust. Flame* 99:43–52 (1994).
- Field, M. A., Gill, D. W., Morgan, B. B., and Hawksley, P. G. W., *Combustion of Pulverized Coal*, Cheney and Sons, Banbury, U.K., 1967.
- Pont, G., Willis, J. W., Karagozian, A. R., and Smith, O. I., *Proc. Combust. Inst.* 26:2463–2470 (1996).
- Willis, J. W., Lee, L.-M., and Karagozian, A. R., *Combust. Sci. Technol.* 94:469–481 (1993).
- Egolfopoulos, F. N., *Proc. Combust. Inst.* 25:1365–1373 (1994).
- Thring, M. W., and Newby, M. P., *Proc. Combust. Inst.* 4:789–796 (1953).
- Schadow, K. C., Gutmark, E., Wilson, K. J., and Smith, R. A., *Fluid Mixing Device Having a Conical Inlet and a Non-Circular Outlet*, U.S. Patent 4,957,242, 1990.

COMMENTS

Friedrich Dinkelacker, University of Erlangen, Germany. For practical applications, is the sound emission to the environment a real problem for these kind of combustors?

Author's Reply. The insulation around a practical system would deaden the sound to some degree, but this system is an ideal candidate for active sound cancellation. The driving signal is known, so an out-of-phase "anti-sound" signal could be generated that would greatly reduce acoustic emissions. However, in the industrial full-scale test en-

vironment the acoustics of the non-insulated actively controlled afterburner was actually minor compared to other industrial noises from compressors, pumps, and so on.

I. Glassman, Princeton University, USA. I would assume that the visible flame height did not vary with increases in the prime fuel jet velocity. Is that so? If so, your flame is simply controlled by simple turbulent jet mixing and the height would be about 6 primary jet air port diameters.

Author's Reply. It is important to note that, unlike the turbulent jet flame, the main jet in this case is air, not fuel, and so the two cases are not entirely analogous. Examining equation 1, which describes vortex shedding frequency, and equation 3, which describes entrainment, it would be concluded that the flame length should not increase with central air jet velocity, much as in the case of the turbulent jet flame. However, prior analysis of this system [Ref. 9 in paper] showed that the mechanism for mixing of the fuel stream, air, and recirculated combustion products is distinctly different from that of a jet diffusion flame. First of

all flame sheet, or flamelet combustion, is not apparent. Secondly, strain-delayed ignition is very important and seems to dominate mixing. That being said, the visible flame height was not strongly controlled by the central air jet velocity, but was controlled by the actively driven vorticity of the central air jet: without the acoustic forcing the flame is yellow and long, with it the flame is blue and short. The fuel stream velocity is secondary: it needed to be near the central air jet velocity to get the best mixing and performance. Lower fuel stream velocities (via larger area) led to reduced entrainment into the acoustically driven vortex and reduced performance.